Behavioural Brain Research 401 (2021) 113079

Contents lists available at ScienceDirect

Behavioural Brain Research

journal homepage: www.elsevier.com/locate/bbr

Microstructural white matter connectivity underlying the attentional networks system

Fernando G. Luna [a,b,1,*], Juan Lupiáñez [b], Elisa Martín-Arévalo [b,**]

[a] Instituto de Investigaciones Psicológicas (IIPsi), CONICET-UNC, Facultad de Psicología, Universidad Nacional de Córdoba, Boulevard de la Reforma esquina Enfermera Gordillo, CP 5000. Córdoba, Argentina

[b] Department of Experimental Psychology, and Mind, Brain, and Behavior Research Center (CIMCYC), University of Granada, Campus de Cartuja S/N, CP 18011, Granada, Spain

ARTICLE INFO

Keywords:
Attentional networks
Diffusion-Weighted Imaging
Alerting
Orienting
Executive control
Vigilance

ABSTRACT

Nowadays, there is considerable controversy regarding the structural connectivity underlying the attentional networks system (i.e., alerting and vigilance, orienting, and executive control). The present study aimed at further examining and dissociating the white matter connectivity underlying attentional and vigilance functioning by overcoming some critical limitations in previous research. To this end, we performed virtual *in vivo* dissections of attention-related white matter tracts from thirty healthy adults. Participants completed two sessions of the Attentional Networks Test for Interactions and Vigilance, a suitable task to assess simultaneously phasic alertness, orienting, executive control, and the executive component of vigilance (i.e., the ability to detect infrequent critical signals). Whereas we found a consistent correlation between phasic alertness and both the right dorsolateral prefrontal caudate tract and the splenium of the corpus callosum, evidence obtained for white matter connectivity underlying orienting, executive control, and executive vigilance, was either weak at the best, inconsistent, or null. White matter connectivity seemed to support nevertheless the most reliable performance: overall reaction time for attentional functioning was significantly associated with the left cingulate fasciculus and overall reaction time for executive vigilance was significantly linked to the bilateral superior longitudinal fasciculus I. The present outcomes provide interesting, consistent, and reliable evidence concerning the structural connectivity underlying the alerting network. We still consider that further evidence is necessary to better understand the controversial relationship between attentional/vigilance processes and microstructural white matter connectivity though.

1. Introduction

Human attentional networks comprise a diverse set of brain circuits supporting attentional performance [1,2]. According to the conventional model proposed by Posner and colleagues, attentional processes are specifically developed by three relatively independent networks which, nevertheless, may interact with each other [1–3]. The alerting network is regulated by norepinephrine innervations from the locus coeruleus towards parietal and prefrontal cortices of the right hemisphere, a set of regions underlying both phasic alertness (i.e., a brief and momentary increment of arousal) and vigilance (i.e., the ability to sustain attention for extended time periods) [4]. The posterior network comprises the superior colliculus and the pulvinar nuclei of the thalamus, along with the frontal eye fields and posterior parietal regions. This network is involved in attentional orienting over spatial sources from the environment to locate potentially relevant stimuli [5]. Finally, the anterior network mainly involves the anterior cingulate and dorsolateral prefrontal cortices, a circuit that underlies executive control

Abbreviations: EV, executive vigilance; ANTI, Attentional Networks Test for Interactions; ANTI-V, Attentional Networks Test for Interactions and Vigilance.

* Corresponding author at: Instituto de Investigaciones Psicológicas (IIPsi), CONICET-UNC, Facultad de Psicología, Universidad Nacional de Córdoba, Boulevard de la Reforma esquina Enfermera Gordillo, CP 5000, Córdoba, Argentina.

** Corresponding author at: Department of Experimental Psychology, and Mind, Brain, and Behavior Research Center (CIMCYC), University of Granada, Campus de Cartuja S/N, CP 18011, Granada, Spain.

E-mail addresses: fluna@unc.edu.ar (F.G. Luna), jlupiane@ugr.es (J. Lupiáñez), emartina@ugr.es (E. Martín-Arévalo).

[1] Permanent address at: Instituto de Investigaciones Psicológicas (IIPsi), CONICET-UNC, Facultad de Psicología, Universidad Nacional de Córdoba, Boulevard de la Reforma esquina Enfermera Gordillo, CP 5000. Córdoba, Argentina

https://doi.org/10.1016/j.bbr.2020.113079
Received 17 June 2020; Received in revised form 21 November 2020; Accepted 14 December 2020
Available online 25 December 2020

processes to direct action towards relevant information to adapt our behavior to long term goals [6,7].

To behaviorally assess the independence of the attentional networks functioning at the same time, Fan et al. developed the Attentional Network Test (ANT) [8]. The ANT combines a visual cueing paradigm [9] suitable to assess the phasic alertness and orienting performance, along with a flanker task [10] that provides an adequate assessment of the executive control network functioning. Importantly, the ANT has demonstrated to be an effective and reliable method to assess the behavioral patterns of attentional components [11,12], and it has been extensively used for examining brain activity (e.g., by mainly using functional magnetic resonance imaging and/or electroencephalography) underlying the attentional networks system [13–19]. At present, nevertheless, to the best of our knowledge, the evidence concerning the specific structural connectivity supporting the attentional networks circuits in healthy adults is both scarce and inconsistent at best [20–24].

In particular, to analyze and determine the structural brain connectivity underlying the human attentional networks, there has been a notable and rising interest in the use of Diffusion-Weighted Imaging (DWI) [25–27]. The reconstruction of the whole-brain tractography from DWI data acquisition is specially adequate to analyze the structural organization and brain connectivity of white matter tracts [28,29]. Indeed, an often-used approach to understanding the relationship between structural white matter tracts connectivity and cognitive functioning is to perform virtual *in vivo* dissections of brain fasciculus/tracts of interest [21,30], and then to offline correlate the indices of white matter connectivity with performance scores [20,25,27,31].

A classical informative index of white matter connectivity is the fractional anisotropy (FA), which ranges from 0 (isotropic diffusion) to 1 (anisotropic diffusion) depending on the diffusion directionality of the molecules within the fibers [29,32]. In general, it has been reported that the higher the FA, the higher the connectivity between the brain regions and therefore, the higher the potential relationship with the cognitive performance [29,33]. Note that, however, a critical limitation of the FA is that it represents average measures of tissue's properties and fibers orientations, not being a fiber-specific index. In this regard, most recent spherical deconvolution methods have been developed to solve this multiple fiber orientations limitation [34] and to improve tractography reconstructions, although its use has not been extensively explored in the assessment of the attentional networks functioning.

The structural connectivity underlying the attentional networks system was previously examined by Niogi et al., by linking the attentional networks' performance measured with the ANT with the white matter connectivity by using the FA index [20]. The authors observed three pairs of positive and independent correlations between (a) the left posterior limb of the internal capsule (PLIC) and phasic alertness, (b) the splenium of the corpus callosum (CC) and attentional orienting, and (c) the anterior corona radiata and executive control. Regarding vigilance, it has been found that the sensitivity to detect infrequent critical targets across time on task in the Continuous Performance Test [35] was positively correlated with the FA index of the right cingulate fasciculus [36]. Furthermore, a different role of the left and right dorsolateral prefrontal caudate (DLPFC) tract was observed for different attentional functions by also using the Continuous Performance Test: whereas the left DLPFC seemed to be involved in executive control processes, the right DLPFC tract was strongly associated with vigilance performance [22].

Importantly, by reconstructing DWI data with the most sensitive spherical deconvolution approach, Thiebaut de Schotten et al. [21] were able to disentangle that the classical white matter tracts related to the visuospatial attentional network would correspond to the superior longitudinal fasciculus (SLF) branches I, II, and III [37]. In particular, the SLF I would be linked to the dorsal attentional network proposed by Corbetta et al. [38], which connects dorsal prefrontal and posterior parietal cortices, and is involved in voluntary orienting of spatial attention towards target stimuli. The SLF III would be overlapped with the right-lateralized ventral frontoparietal attentional network, underlying the automatic capture of spatial cues [38]. Lastly, the SLF II would be a white matter tract connecting the dorsal prefrontal regions of the SLF I and the parietal regions of the SLF III [21,39]. Note that the SLFs (especially those with rightward hemispheric lateralization) were correlated with the behavioral degree of leftward bias during tasks assessing visuospatial attention [21].

1.1. The present study

Taking all the above into account, it is important to highlight that previous research has (a) analyzed the structural brain connectivity of attentional networks in healthy adults examining attentional and vigilance performance across separated studies, and (b) used the traditional FA index as a proxy of white matter connectivity, in most cases [20–22,36]. To overcome these limitations, the present study aimed at further examining the microstructural white matter connectivity underlying multiple cognitive components of the attentional networks system [25,26] by using the highly sensitive spherical deconvolution approach [34]. Thus, to this end, we offline correlated data from (a) virtual *in vivo* dissections of white matter tracts previously reported as related to attentional and vigilance performance [20–22,36], and (b) performance scores computed from a new version of the classic ANT, i.e., the ANT for Interactions and Vigilance (ANTI-V) [40]. Importantly, note that the ANTI-V is a task suitable to assess in a single session the independence and interactions of the classic attentional components (i.e., phasic alertness, orienting, and executive control) as the ANT for Interactions (ANTI) developed by Callejas et al. [41] along with an executive component of vigilance (EV), i.e., the maintenance of attention over long time periods for detecting rare but critical signals [40,42–44]. We expect the present study to contribute to a better understanding of the white matter connectivity underlying the human attentional networks in healthy adults [1,25,26].

2. Material and methods

2.1. Participants

A total of thirty undergraduate students (16 women, age: $M = 18.57$; $SD = 4.12$) from the University of Granada, Spain, volunteered to participate in the study in exchange for monetary compensation (10 Euros/h). Participants signed an informed consent approved by the local ethics committee and completed a safety protocol for magnetic resonance imaging (MRI) data acquisition. All participants had normal or corrected to normal vision and none of them had a history of neurological illness. The present study was conducted according to the ethical standards of the 1964 Declaration of Helsinki (last update: Seoul, 2008) and it was part of a larger research project, which was positively evaluated by the University of Granada Ethical Committee (PSI2014-52764-P).

2.2. Diffusion-weighted imaging

2.2.1. Data acquisition

A total of 70 near-axial slices were acquired on a Siemens 3-TRIO TIM system –equipped with a 32-channel head coil– at the Brain, Mind, and Behaviour Research Center (CIMCYC), University of Granada. We used a sequence fully optimized for DWI of white matter (based on Damped Richardson Lucy Spherical Deconvolution) [34], providing isotropic ($2 \times 2 \times 2$ mm) resolution and coverage of the whole head with a posterior-anterior phase of acquisition (echo time =88 ms and repetition time =8400 ms). Note that Damped Richardson Lucy Spherical Deconvolution estimates multiple orientations in voxels containing different populations of crossing fibers [45,46]. At each slice location, 6 images were acquired with no diffusion gradient applied and 60 diffusion-weighted images in which gradient directions were uniformly distributed in space. The diffusion weighting was equal to a b-value of

1500s/mm^2.

2.2.2. Data pre-processing and virtual in vivo dissections

DWI data processing were performed following similar previously reported procedures [20–22,30,47]. First, and for each slice, diffusion-weighted data were simultaneously registered and corrected for participant motion and geometrical distortion adjusting the gradient accordingly by using the ExploreDTI toolbox [48] on MATLAB R2017a (The MathWorks, Inc.). Then, individual dissections were carried out with the software TrackVis [49]. Based on previous DWI researches on attention and vigilance, the following white matter tracts of interest were selected: the three branches of the SLF [21,31,37,38], the splenium of the CC and the PLIC [20], the cingulate fasciculi [36], and the DLPFC [22]. All white matter tracts were virtually dissected by using a single/multiple Regions of Interest (ROI) approach based on methodological procedures reported in previous studies, as described below. Fig. 1 shows all ROIs and reconstructed targeted tracts (i.e., SLFs, cingulate fasciculus, splenium of the CC, PLIC tracts, and DLPFC tracts) in the left hemisphere, as an example in one representative participant per tract.

The three branches of the SLF (on both the left and right hemisphere) were isolated by using a multiple-ROI approach, as in Thiebaut de Schotten et al. [21]. Parietal ROIs and frontal ROIs were delineated around the white matter, based on the guidelines provided in Thiebaut de Schotten et al. [21]. A not-part ROI in the temporal and the CC white matter were also used to exclude streamlines of the arcuate fasciculus projecting to the temporal lobe [21,50]. The two cingulate fasciculi (on both the left and right hemisphere) were isolated by using an one-ROI approach, as recommended in Catani and Thiebaut de Schotten [30], with a not-part ROI in the CC white matter to avoid crossing fibers. The splenium of the CC was also isolated by using an one-ROI approach, based on Catani and Thiebaut de Schotten [30,47]. The PLIC (on both the left and right hemisphere) were isolated by using a multiple-ROI approach, based on Niogi et al. [20], with a not-part ROI in the CC white matter. Finally, the DLPFC tract (on both the left and right hemisphere) were isolated by using a multiple-ROI approach, as recommended in Chiang et al. [22]. A ROI in the dorsolateral prefrontal cortex and a ROI in the caudate nucleus were delineated around the white matter, with a not-part ROI in the CC white matter.

The index employed as a surrogate for tract microstructural organization (i.e., the mean Hindrance Modulated Orientational Anisotropy –HMOA–) [34] was extracted from each dissected tract. The mean HMOA is defined as the absolute amplitude of each lobe of the fibers orientation distribution within a specific white matter orientation, and it is considered highly sensitive to axonal myelination, fiber diameter, and axonal density [34], providing specific information about the distinct fibers orientations. Thus, whereas the lowest value (i.e., 0) of HMOA indicates the absence of fibers, the highest value (i.e., 1) corresponds to a signal that references the highest fibers orientation distribution amplitude that can be realistically detected in a specific white matter orientation [34]. Note that a relevant advantage of the HMOA index is that it can be used to describe the microstructural properties of a single fiber population that are dissected from voxels containing multiple fiber orientations with different tissue properties (e.g., such as the axonal diameter or the degree of myelination) [34].

2.3. Behavioral Assessment: ANTI-V

Participants completed two experimental sessions of the ANTI-V task [40], one before and the other after MRI data acquisition. The task was designed and run in E-Prime v2.0 Professional [Psychology Software Tools, Pittsburgh, PA, [51]], and responses were registered with a standard QWERTY keyboard. In short, the ANTI-V combines two embedded tasks: (a) in the largest proportion of trials (i.e., 75 %), participants have to complete the ANTI task [41], which is suitable to assess the independence and interactions of the classic attentional functions; and (b) in the remaining trials (i.e., 25 %), participants perform a signal-detection task similar to the Continuous Performance Test [35] that is suitable to assess EV. The stimuli sequence and timing for the ANTI and EV trials are depicted in Fig. 2, and are described in detail in Roca et al. [40].

In the ANTI trials, participants completed a flanker task by responding to the direction the target (i.e., a central arrow) pointed to, while ignoring the surrounding flanking arrows. To assess executive control, in half of these trials the direction of the target pointed to the same direction than distractors (congruent condition), whereas in the other half it pointed to the opposite direction (incongruent condition). To assess phasic alertness, a warning signal could anticipate the response stimuli in half of these trials (tone condition), while no warning signal was presented in the other half (no tone condition). Finally, to assess attentional orienting, an exogenous visual cue could be presented above or below the fixation point before the string of arrows. In particular, the visual cue could (a) appear at the same location as the response' stimuli (33.3 % of times, valid cue condition), (b) at the opposite location (33.3 % of trials, invalid condition), or (c) not be presented (33.3 % of trials, no cue condition). Examples of visual cue and congruency are depicted in Fig. 2.

As above-mentioned, the EV task was embedded along with the ANTI trials, and it demanded to perform a signal-detection task similar to the Continuous Performance Test [35]. In short, the EV trials (i.e., 25 %) had the same procedure than the ANTI ones, except that the target was horizontally displaced from its central position (either leftwards or rightwards, see Fig. 2). Participants were instructed to remain vigilant to detect the large displacement by pressing the space bar while ignoring in these cases the direction pointed by the target.

Before the experiment task, participants received specific instructions to correctly perform the different types of trials, and then they completed one practice block of 64 randomized trials (48 ANTI and 16 EV) with visual feedback. Afterward, they completed 6 experimental blocks of 64 randomized trials (48 ANTI and 16 EV per block), with no pause nor visual feedback. The 48 ANTI trials had the following factorial design: Warning signal (no tone/tone) × Visual Cue (invalid/no cue/valid) × Congruency (congruent/incongruent). The 16 EV trials per block were randomly selected from all the possible trial combinations.

2.4. Statistical analyses

Repeated-measures analysis of variance (ANOVA) and bivariate Pearson correlations were conducted in Statistica 8.0 [52], and JASP [53] was used to perform Bayesian correlations [54]. One participant was excluded due to an extreme overall percentage of errors in the ANTI trials (3 *SD* above the group mean), and two participants were additionally excluded due to technical errors in the DWI reconstruction, thus leaving a final sample of twenty-seven participants.

2.4.1. Attentional networks performance

A first analysis examined whether the independence and interactions of the classic attentional functions were successfully observed in the present study, as expected with the ANTI [41,55] and ANTI-V [40,42] tasks. For the ANTI trials, the reaction time (RT) analyses excluded trials with incorrect responses (7.29 %) and with RT below 200 ms or above 1500 ms (0.76 %). The main effects and interactions of the classic attentional components included two repeated-measures ANOVAs, with RT and percentage of errors as dependent variable, respectively, and including warning signal (no tone/tone), visual cue (invalid/no

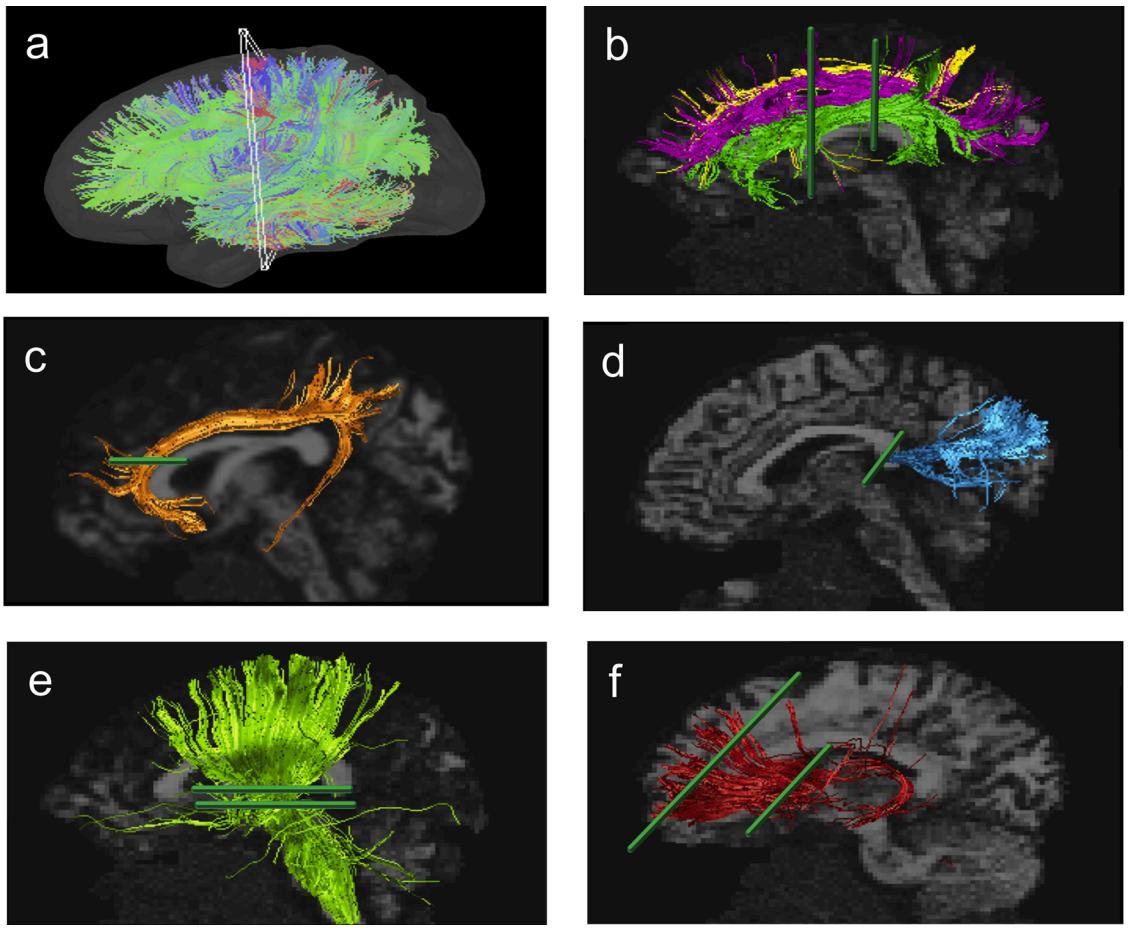

Fig. 1. Example of reconstructions in TrackVis software in sagittal view – left hemisphere, as an example in one representative participant per tract: (a) reconstruction of the whole-brain tractography. The different colors represent the direction of the reconstructed fibers: in green the fibers with antero-posterior direction, in red with left-right direction, and in blue with dorsal-ventral direction. (b) SLFs tracts. (c) cingulate fasciculus tract. (d) splenium of the CC tract. (e) PLIC tract. (f) DLPFC tract. Green lines represent the Regions of Interest (ROIs) per tract. The colors of the tracts (images b to f) were randomized for visualization.

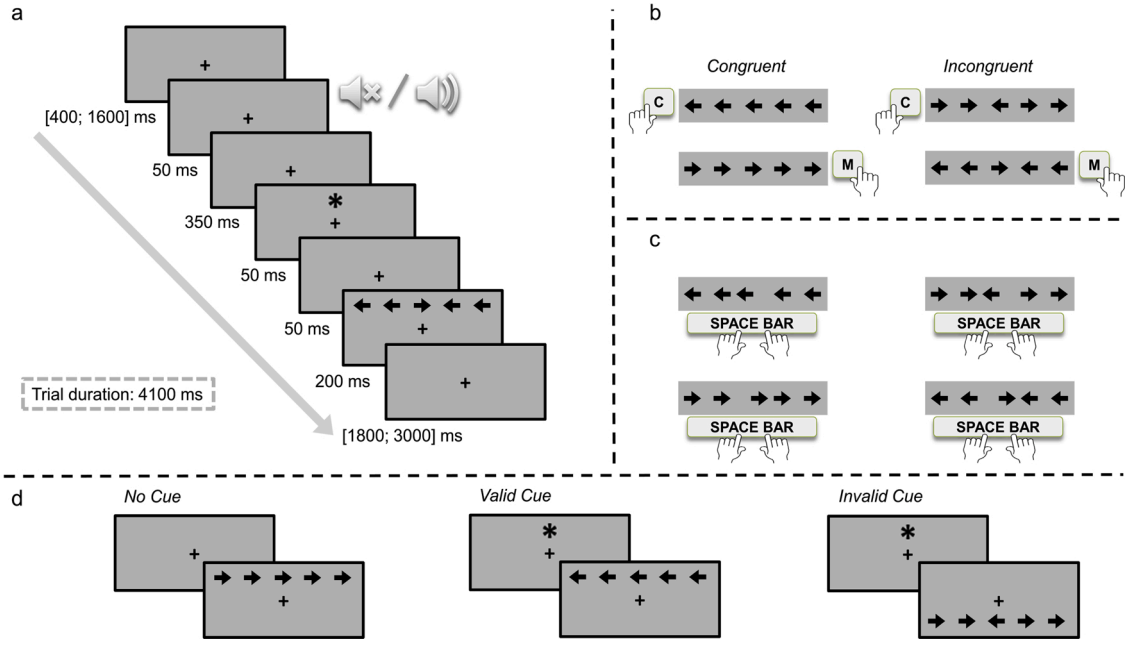

Fig. 2. Procedure and conditions for the trials of the ANTI-V task. (a) Stimuli timing and sequence for both ANTI and EV trials. Responses were allowed until 2000 ms since the target appearance. (b) Examples of congruency conditions. (c) Examples of target displacement in EV trials. Panels (b) and (c) show the correct response for each type of ANTI and EV trials. (d) Examples of visual cue conditions.

cue/valid), congruency (congruent/incongruent), and session (two levels) as within-participant factors.

2.4.2. Attentional and EV reliability scores

We then analyzed the test-retest reliability by Pearson's bivariate correlations between the two experimental sessions.[2] We computed the attentional networks scores proposed by Callejas et al. [41] by subtracting average data in specific conditions. In particular, the phasic alertness score (i.e., the difference between no tone minus tone conditions) was computed in two different ways: (a) considering all trials, and (b) only including trials with no visual cue, i.e., wherein alertness seems to increase its effect [41]; although note that this score might be less reliable as it is computed from fewer observations. For attentional orienting, we computed three different scores: (a) the orienting score, as the result of invalid minus valid conditions; (b) the benefits score (i.e., no cue minus valid conditions), which refers to the orienting enhancement obtained from valid visual cues; and (c) the costs score (i.e., invalid minus no cue conditions), as the impairment in orienting as consequence of invalid visual cues. The executive control score was obtained as the difference between incongruent and congruent conditions. Finally, we also computed overall scores for both RT and percentage of errors.

For the EV trials, warning tone, visual cue, and congruency levels were not considered for analyses, with data being collapsed across all these variables. We computed the following signal-detection theory metrics: hits (i.e., correct responses in the EV trials) and false alarms (i.e., space bar responses in the ANTI trials) rate, and non-parametric indices of sensitivity (A′) and response bias (B″) [56]. Additionally, we obtained the mean and *SD* of RT on hits, excluding trials with a RT below 200 ms or above 1500 ms (2.02 %).

2.4.3. Correlations between behavioral and DWI data

Bivariate correlations were performed between the HMOA index obtained from each virtual *in vivo* dissected tract, and the overall scores computed across sessions of the classic attentional components and EV. Note that, importantly, correlations were performed by using two different statistical approaches. While Null-Hypothesis Significance Testing (NHST, i.e., Pearson correlations) were conducted for testing statistical significance to reject the null hypothesis (H_0; i.e., the absence of correlation between variables), Bayesian correlations were performed to test the strength of the evidence supporting either H_0 or the alternative hypothesis (H_1; the existence of a positive or negative correlation between variables) [54].[3] Note that, given that thirteen (i.e., the amount of HMOA indices) correlational tests were performed on each attentional/vigilance score, the standard significance level (i.e., $p < .05$) for Pearson correlations was adjusted by Bonferroni correction, being therefore set at $p < .004$.

3. Results

3.1. Attentional networks performance

The main effects of the classic attentional components usually reported with the ANTI [41] and ANTI-V [40] tasks were also found as significant here. The main effect of warning was observed as significant for RT [F (1, 26) = 23.23, $p < .001$, $\eta_p^2 = .47$] and as marginal for errors [F (1, 26) = 4.14, $p = .052$, $\eta_p^2 = .14$]). As depicted in Fig. 3, responses were faster and more precise in the tone than no tone condition. The main effect of visual cue was significantly observed only for RT [F (2, 52) = 53.81, $p < .001$, $\eta_p^2 = .67$], but not for errors ($F < 1$). As observed in Fig. 3, the visual cueing effect was found as usually observed: responses were faster in the valid than in the no cue condition, and faster in this than in the invalid condition, therefore respectively showing significant attentional benefits [F (1, 26) = 24.81, $p < .001$, $\eta_p^2 = .49$] and costs [F (1, 26) = 23.39, $p < .001$, $\eta_p^2 = .47$] effects. Lastly, the congruency effect was significantly observed for both RT [F (1, 26) = 268.85, $p < .001$, $\eta_p^2 = .91$] and errors [F (1, 26) = 40.47, $p < .001$, $\eta_p^2 = .61$]. As expected, responses were faster and more accurate in the congruent than incongruent condition (see Fig. 3).

Moreover, the two-way interactions usually reported with the ANTI [41] and ANTI-V [40] tasks were also found as significant here (see Table 1): Warning signal × Visual cue (RT [F (2, 52) = 7.96, $p < .001$, $\eta_p^2 = .23$]; errors [F (2, 52) = 4.05, $p = .023$, $\eta_p^2 = .13$]), Warning signal × Congruency (only for RT [F (1, 26) = 8.39, $p = .008$, $\eta_p^2 = .24$]; not for errors, $F < 1$), and Visual cue × Congruency (only for RT [F (2, 52) = 8.54, $p < .001$, $\eta_p^2 = .25$]; not for errors [F (2, 52) = 2.11, $p = .131$, $\eta_p^2 = .08$]). Altogether, this pattern of outcomes further demonstrates that the ANTI-V task was suitable to assess both the independence and the interactions of the classic attentional components in the present study.

Importantly, as can be observed in Table 1, there was not a significant main effect of experimental session for both RT and errors (both Fs < 1.05, ps $< .320$). Moreover, the experimental session did not significantly modulate any of the main effects of the classic attentional components: warning signal (RT [F (1, 26) = 1.66, $p = .209$, $\eta_p^2 = .06$], errors [F (1, 26) = 3.83, $p = .061$, $\eta_p^2 = .13$]), visual cue (RT [F (2, 52) = 2.11, $p = .132$, $\eta_p^2 = .07$], errors [F (2, 52) = 1.34, $p = .271$, $\eta_p^2 = .05$]), and congruency (RT, $F < 1$; errors [F (1, 26) = 1.41, $p = .246$, $\eta_p^2 = .05$]).

3.2. Test-retest reliability

As can be observed in Table 2, the overall RT of the ANTI trials showed high reliability score, whereas it was found moderate reliability for executive control and phasic alertness (only in the RT score computed for all trials) and low reliability for the orienting scores and the overall percentage of errors. Note that these outcomes were observed in the same vein that previous studies appraising the reliability of the ANT [11] and ANTI-V [42] tasks. Importantly, moderate to high reliabilities were found for the EV indices, as previously reported with the split-half method for the ANTI-V [42], thus proving that the task was suitable to obtain an independent measure of EV across sessions.

3.3. Descriptive statistics of white matter tracts

Table 3 shows the descriptive statistics of the HMOA index for each of the targeted virtual *in vivo* dissected tracts. To control for the dissections reliability, we compared the HMOA indices between hemispheres –for the well-known lateralized tracks– based on previous data [20–22,30,47]. Supporting previous outcomes [21], there was a significant right lateralization for the SLF II [t (26) = 4.95, $p < .001$] and SLF III [t (26) = 3.32, $p = .003$], which was not observed for the SLF I [t (26) = 0.20, $p = .840$]. In addition, and also in the same vein that previous findings [58,59], both the cingulate fasciculus [t (26) = 4.20, $p < .001$] and the PLIC [t (26) = 5.80, $p < .001$] were left lateralized. Lastly, and also in line with previous findings [22], the DLPFC showed no lateralization between hemispheres [t (26) = 1.27, $p < .217$]. Thus, the usual

[2] Note that, according to MacLeod et al. [11], a practical interpretation –for research purposes– of the reliability based on the test-retest correlations scores might be that (a) values smaller than .40 reflect low reliability; (b) values between .40 and .60 might be interpreted as moderate reliability; (c) value between .60 and .70 can be considered as moderate-high reliability; and (d) values greater than .70 can be considered as high reliability.

[3] Note that the inverse Bayes Factor (BF_{10}) might be interpreted as described by Jarosz and Wiley [60] as (a) below 0.33, as consistent evidence in favor for the H_0; (b) between 0.33 and 1, as inconsistent evidence supporting neither the H_0 nor the H_1; (c) between 1 and 3, as anecdotal evidence for the H_1; (d) above 3, as consistent evidence supporting the H_1, and in particular: between 3 and 10 as substantial, between 10 a 30 as strong, between 30 and 100 as very strong, and above 100 as decisive evidence for the H_1.

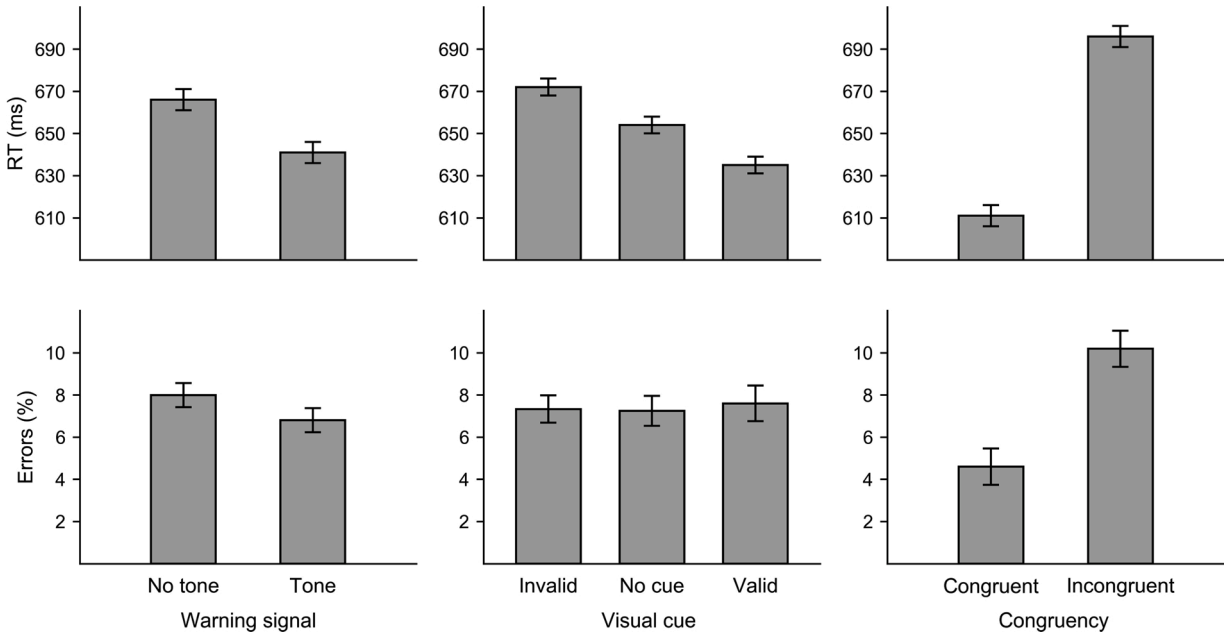

Fig. 3. Mean correct RT (superior panels) and percentage of errors (lower panels) for the warning signal, visual cue, and congruency conditions (data collapsed across the two sessions). Error bars represent 95 % confidence interval and were computed following the method developed by Cousineau [57].

Table 1
Mean correct RT (ms) and percentage of errors for the phasic alertness, visual cue, and congruency conditions, as a function of experimental sessions.

			Session 1				Session 2			
			Congruent		Incongruent		Congruent		Incongruent	
			M	95 % CI	*M*	95 % CI	*M*	95 % CI	*M*	95 % CI
Reaction time										
	No tone	Invalid	632	[595, 668]	719	[679, 759]	635	[590, 681]	719	[671, 768]
		No cue	639	[603, 674]	712	[673, 752]	640	[592, 688]	704	[660, 748]
		Valid	609	[573, 645]	688	[647, 728]	611	[565, 658]	690	[636, 745]
	Tone	Invalid	615	[582, 648]	716	[683, 749]	609	[558, 660]	733	[680, 787]
		No cue	603	[569, 637]	669	[633, 705]	585	[539, 632]	677	[629, 725]
		Valid	588	[556, 620]	675	[634, 717]	570	[527, 614]	651	[604, 699]
Errors										
	No tone	Invalid	4.17	[1.62, 6.71]	11.57	[8.11, 15.04]	6.17	[2.90, 9.45]	12.04	[7.97, 16.11]
		No cue	3.55	[1.32, 5.78]	8.95	[5.93, 11.97]	6.48	[3.02, 9.94]	13.12	[8.09, 18.14]
		Valid	4.01	[2.16, 5.87]	9.26	[6.47, 12.05]	6.02	[2.30, 9.74]	10.49	[6.80, 14.19]
	Tone	Invalid	1.08	[0.10, 2.06]	9.41	[5.80, 13.03]	4.94	[1.87, 8.01]	9.26	[5.43, 13.09]
		No cue	3.24	[1.23, 5.25]	8.80	[5.27, 12.32]	4.32	[1.45, 7.19]	9.57	[5.86, 13.28]
		Valid	5.56	[2.74, 8.37]	10.49	[7.09, 13.90]	5.71	[2.38, 9.04]	9.26	[5.51, 13.01]

Note. M = mean, CI = confidence interval.

lateralization pattern of tracts was also observed in the present study.

3.4. Correlations between attentional and EV scores and white matter connectivity

For the sake of clarity, correlations matrices between performance scores and DWI data are presented in separate tables. For executive control, as can be observed in Table 4, Pearson correlations observed for both RT and errors scores did not reach the corrected significance level and, importantly, none correlation was observed by Bayesian analysis –at least– as positive evidence in favor of the existence of correlation [60]. However, as can be also observed in Table 4, a negative correlation (r = -.47, $p < .05$) between the left cingulate fasciculus and the overall RT, showing that the higher the HMOA, the faster the responses for the ANTI task. Note that, in this case, this negative Pearson correlation was observed by the Bayesian analysis as positive evidence for the existence of correlation (BF_{10} = 4.49).

For phasic alertness, as can be observed in Table 5, negative Pearson correlations between the errors score (computed only from the no cue trials) with the HMOA of the right DLPFC (r = -.53, $p < .005$; BF_{10} = 10.44) and the splenium of the CC (r = -.54, $p < .004$; BF_{10} = 13.59) were also observed as strong evidence for the existence of correlation by the Bayesian analysis. Moreover, the errors score computed from all trials showed an even stronger significant negative correlation with the splenium of the CC, also observed as very strong evidence in favor of the existence of correlation by the Bayesian analysis (r = -.61, $p < .001$; BF_{10} = 54.70). Thus, the higher the HMOA index of both the right DLPFC and especially the splenium of the CC, the smaller the effect of phasic alertness on performance. Finally, note that, however, previous correlations found between the left PLIC and phasic alertness [20] were observed in the present study as non-significant and, at the same time, demonstrated either consistent evidence in favor of the absence of a correlation (for the RT scores) or inconsistent evidence for either the H_0 or the H_1 (for the errors scores).

For the orienting network, although it was highly expected to be associated with both the right SLF III [21] and the splenium of the CC

Table 2
Attentional and executive vigilance performance scores for each experimental session, the overall across sessions, and the test-retest reliability scores between sessions.

	Session 1	Session 2	Overall	Test-retest
	M [95% CI]	*M* [95% CI]	*M* [95% CI]	*r* Pearson
ANTI - Reaction Time (ms)				
Overall	654 [620, 687]	651 [605, 697]	651 [615, 687]	.70****
Phasic alertness	22 [10, 34]	29 [17, 41]	25 [15, 36]	.56***
Phasic alertness (no cue)	39 [22, 55]	40 [21, 60]	39 [23, 55]	.42*
Orienting	29 [21, 37]	43 [33,52]	36 [30, 42]	.03
Benefits	16 [7, 24]	20 [9, 31]	18 [10, 25]	.24
Costs	13 [2, 24]	22 [11, 34]	18 [10, 26]	.10
Executive control	82 [70, 94]	87 [75, 99]	85 [74, 95]	.59***
ANTI - Errors (%)				
Overall	6.67 [4.82, 8.53]	8.11 [5.20, 11.03]	7.39 [5.42, 9.37]	.33
Phasic alertness	0.49 [-0.79, 1.77]	1.88 [0.37, 3.39]	1.18 [-0.01, 2.38]	.46*
Phasic alertness (no cue)	0.23 [-1.77, 2.23]	2.85 [0.25, 5.46]	1.54 [-0.36, 3.45]	.36
Orienting	−0.77 [-2.66, 1.12]	0.23 [-1.22, 1.68]	−0.27 [-1.65, 1.11]	.36
Benefits	−1.20 [-3.10, 0.71]	0.50 [-1.08, 2.08]	−0.35 [-1.82, 1.13]	.43*
Costs	0.42 [-1.59, 2.43]	−0.27 [-1.62, 1.08]	0.08 [-1.06, 1.21]	−.13
Executive control	6.15 [4.45, 7.84]	5.02 [2.66, 7.37]	5.58 [3.78, 7.38]	.57***
Executive vigilance				
Mean RT (ms)	852 [811, 894]	850 [804, 895]	852 [811, 894]	.85****
SD of RT (ms)	151 [134, 167]	150 [132, 168]	152 [137, 166]	.65****
Hits (%)	48.50 [41.30, 55.69]	44.79 [37.53, 52.05]	46.64 [39.69, 53.60]	.85****
False alarms (%)	4.21 [2.64, 5.77]	4.24 [2.71, 5.78]	4.22 [2.86, 5.59]	.54***
Sensitivity (A')	0.84 [0.82, 0.87]	0.83 [0.81, 0.85]	0.84 [0.81, 0.86]	.85****
Response Bias (B″)	0.72 [0.62, 0.81]	0.71 [0.62, 0.80]	0.71 [0.63, 0.79]	.66****

Note. *M* = mean, CI = confidence interval, *r* = Pearson correlation.
* $p < .05$.
*** $p < .005$.
**** $p < .001$.

Table 3
Mean and 95 % confidence intervals of the HMOA index obtained for each white matter tract.

	HMOA	
	Mean	95 % CI
SLF I left	.068	[.064, .072]
SLF I right	.068	[.064, .072]
SLF II left	.083	[.079, .088]
SLF II right	.095	[.091, .099]
SLF III left	.089	[.086, .093]
SLF III right	.093	[.090, .096]
Cingulate left	.124	[.117, .130]
Cingulate right	.113	[.108, .118]
PLIC left	.131	[.127, .134]
PLIC right	.122	[.118, .126]
DLPFC left	.097	[.094, .100]
DLPFC right	.094	[.090, .098]
Splenium CC	.182	[.172, .192]

Note. SLF = superior longitudinal fasciculus, PLIC = posterior limb of internal capsule, DLPFC = dorsolateral prefrontal caudate, CC = corpus callosum, HMOA = Hindrance Modulated Orientational Anisotropy, CI = confidence interval.

Table 4
Bivariate Pearson and Bayesian correlations between overall and executive control scores, and the HMOA index of each targeted white matter tract.

	Reaction Time scores				Errors scores			
	Overall		Executive control		Overall		Executive control	
	r	BF_{10}	*r*	BF_{10}	*r*	BF_{10}	*r*	BF_{10}
SLF I left	−.18	0.35	−.15	**0.31**	.04	**0.24**	.13	**0.29**
SLF I right	−.18	0.35	−.30	0.71	.12	**0.28**	.19	0.37
SLF II left	−.43	2.49	−.27	0.57	−.14	**0.30**	.08	**0.26**
SLF II right	.08	**0.26**	.01	**0.24**	−.01	**0.24**	.01	**0.24**
SLF III left	−.15	0.32	−.17	0.34	−.03	**0.24**	.13	**0.29**
SLF III right	.09	**0.26**	.06	**0.25**	−.03	**0.24**	.16	**0.32**
Cingulate left	−.47	**4.49**	−.27	0.60	−.17	0.33	.07	**0.25**
Cingulate right	−.32	0.84	−.41	1.95	−.08	**0.26**	.07	**0.25**
PLIC left	−.24	0.48	−.12	**0.29**	.13	**0.30**	.38	1.52
PLIC right	.07	**0.25**	−.02	**0.24**	.22	0.44	.38	1.52
DLPFC left	.10	**0.27**	.41	1.97	−.01	**0.24**	.12	**0.28**
DLPFC right	−.37	1.30	.03	**0.24**	−.15	**0.31**	−.03	**0.24**
Splenium CC	−.19	0.37	−.05	**0.25**	.18	0.35	.28	0.64

Note. Inverse Bayes factors (BF_{10}) supporting the H_0 (i.e., < 0.33) are presented in boldface, while those supporting the H_1 (i.e., > 3) are presented in boldface and underlined. SLF = superior longitudinal fasciculus, PLIC = posterior limb of internal capsule, DLPFC = dorsolateral prefrontal caudate, CC = corpus callosum, *r* = Pearson correlation, BF = Bayes Factor.

[20], the correlations observed in Table 6 in the errors score did not reach the corrected significance level and did not show at least positive evidence in favor of the existence of correlation by the Bayesian analysis.

Finally, regarding the scores computed for EV performance, only the overall mean RT on hits showed a negative correlation with both the left (r = -.53, $p < .005$; $BF_{10} = 11.92$) and the right (r = -.50, $p < .01$; BF_{10} = 6.67) SLF I, being both correlations observed as strong and substantial evidence for the existence by the Bayesian analysis, respectively. Thus, the higher the HMOA of bilateral SLF I, the faster the responses for hits on infrequent target detection. Note that, however, signal-detection theory metrics computed for EV did not show any relevant correlation with the HMOA indices of the white matter tracts dissected in the present study (see Table 7).

It is important to note that Bayesian analyses were useful to examine two critical issues of the correlations performed between HMOA indices and the attentional/vigilance scores, which are indeed unable to be addressed by the NHST approach. On the one hand, the inverse Bayes factor demonstrated that a large number of correlations (either unexpected or expected based on previous research [20–22,36]) was observed as consistent evidence in favor of the H_0, i.e., absence of correlation. For instance, whereas Niogi et al. [20] found a positive and significant correlation between the left PLIC and the RT score of phasic alertness, this correlation was observed in the present study for both RT scores of phasic alertness with a $BF_{10} < 0.33$, which rather means evidence in favor of the absence of correlation (see Table 5, but also Tables 4–7 for others correlations with a similar BF_{10}). On the other hand, note that a small but interesting set of outcomes were observed by Bayesian analyses only as anecdotal evidence in favor of the H_1; e.g., the correlations between (a) the left DLPFC and the RT score of executive control, which was previously reported by Chiang et al. [22], was observed here with a $BF_{10} = 1.97$ (see Table 4), although showing an unusual positive correlation; or (b) the right SLF III and the RT orienting score, an association consistently observed in previous studies [21,24,31,39], was observed in the present study with a $BF_{10} = 1.30$ (see Table 6). These data seem to indicate that larger amount of evidence –at least as in the way it is addressed here– is still necessary to further determine whether the correlations observed with anecdotal evidence in favor of the existence of correlation can be effectively supported by

Table 5
Bivariate Pearson and Bayesian correlations between phasic alertness scores, and the HMOA index of each targeted white matter tract.

	Reaction time scores				Errors scores			
	Phasic alertness		Phasic alertness (no cue)		Phasic alertness		Phasic alertness (no cue)	
	r	BF_{10}	*r*	BF_{10}	*r*	BF_{10}	*r*	BF_{10}
SLF I left	.06	**0.25**	.08	**0.26**	−.07	**0.25**	−.16	**0.32**
SLF I right	.06	**0.25**	.14	**0.30**	−.19	0.37	−.19	0.37
SLF II left	.09	**0.26**	.09	**0.26**	−.18	0.35	−.19	0.37
SLF II right	.30	0.71	.23	0.45	.11	**0.27**	.08	**0.26**
SLF III left	.24	0.46	.19	0.36	−.10	**0.27**	.10	**0.27**
SLF III right	.37	1.33	.29	0.64	−.10	**0.27**	.08	**0.26**
Cingulate left	.31	0.76	.33	0.89	−.17	0.34	−.23	0.44
Cingulate right	.25	0.51	.25	0.50	−.28	0.63	−.14	**0.31**
PLIC left	.11	**0.28**	.06	**0.25**	−.18	0.35	−.33	0.93
PLIC right	.38	1.48	.24	0.49	.00	**0.24**	−.14	**0.30**
DLPFC left	.38	1.40	.43	2.49	−.08	**0.26**	−.27	0.56
DLPFC right	−.08	**0.26**	−.02	**0.24**	−.23	0.45	−.53	**10.44**
Splenium CC	.21	0.40	.32	0.84	−.61*	**54.70**	−.54*	**13.59**

Note. Inverse Bayes factors (BF_{10}) supporting the H_0 (i.e., < 0.33) are presented in boldface, while those supporting the H_1 (i.e., > 3) are presented in boldface and underlined. SLF = superior longitudinal fasciculus, PLIC = posterior limb of internal capsule, DLPFC = dorsolateral prefrontal caudate, CC = corpus callosum, *r* = Pearson correlation, BF = Bayes Factor.

* Bonferroni corrected $p < .004$.

Table 6
Bivariate Pearson and Bayesian correlations between the scores computed for the orienting network, and the HMOA index of each targeted white matter tract.

	Reaction time scores						Errors scores					
	Orienting		Benefits		Costs		Orienting		Benefits		Costs	
	r	BF_{10}	*r*	BF_{10}	*r*	BF_{10}	*r*	BF_{10}	*r*	BF_{10}	*r*	BF_{10}
SLF I left	−.02	**0.24**	.03	**0.24**	−.05	**0.25**	−.04	**0.24**	−.29	0.66	.32	0.87
SLF I right	.02	**0.24**	−.20	0.39	.20	0.39	−.23	0.44	−.41	2.10	.26	0.54
SLF II left	−.14	**0.30**	.12	**0.28**	−.21	0.41	.04	**0.24**	−.22	0.42	.33	0.95
SLF II right	−.32	0.86	−.16	0.33	−.09	**0.27**	−.02	**0.24**	−.13	**0.29**	.15	**0.31**
SLF III left	−.23	0.44	−.11	**0.27**	−.07	**0.25**	.07	**0.25**	.03	**0.24**	.05	**0.25**
SLF III right	−.37	1.30	−.21	0.40	−.09	**0.26**	.14	**0.30**	.27	0.59	−.18	0.35
Cingulate left	−.07	**0.25**	−.05	**0.25**	.00	**0.24**	.13	**0.29**	−.02	**0.24**	.18	0.35
Cingulate right	.03	**0.24**	.01	**0.24**	.02	**0.24**	.21	0.41	.00	**0.24**	.26	0.55
PLIC left	−.14	**0.30**	−.04	**0.25**	−.06	**0.25**	.34	1.04	.23	0.44	.12	**0.29**
PLIC right	−.22	0.42	−.23	0.46	.05	**0.25**	.39	1.60	.07	**0.25**	.38	1.47
DLPFC left	−.29	0.68	−.18	0.35	−.06	**0.25**	−.04	**0.24**	.02	**0.24**	−.08	**0.26**
DLPFC right	−.07	**0.25**	.08	**0.26**	−.12	**0.28**	−.08	**0.26**	−.01	**0.24**	−.08	**0.26**
Splenium CC	−.23	0.44	.16	0.33	−.32	0.86	.02	**0.24**	−.11	**0.28**	.17	0.34

Note. Inverse Bayes factors (BF_{10}) supporting the H_0 (i.e., < 0.33) are presented in boldface, while those supporting the H_1 (i.e., > 3) are presented in boldface and underlined. SLF = superior longitudinal fasciculus, PLIC = posterior limb of internal capsule, DLPFC = dorsolateral prefrontal caudate, CC = corpus callosum, *r* = Pearson correlation, BF = Bayes Factor.

Table 7
Bivariate Pearson and Bayesian correlations between the scores computed for executive vigilance, and the HMOA index of each targeted white matter tract.

	Executive Vigilance scores											
	Mean RT		SD of RT		Hits		False alarms		A′		B″	
	r	BF_{10}	*r*	BF_{10}	*r*	BF_{10}	*r*	BF_{10}	*r*	BF_{10}	*r*	BF_{10}
SLF I left	−.53	**11.92**	−.38	1.43	.15	**0.31**	.28	0.61	.12	**0.29**	−.19	0.37
SLF I right	−.50	**6.67**	−.34	0.98	.28	0.62	.34	1.00	.23	0.44	−.25	0.51
SLF II left	−.35	1.14	−.26	0.56	−.26	0.53	−.11	**0.28**	−.16	**0.32**	.12	**0.28**
SLF II right	−.03	**0.24**	.16	**0.32**	.08	**0.26**	.09	**0.26**	.04	**0.24**	−.09	**0.26**
SLF III left	−.11	**0.27**	.05	**0.25**	−.24	0.48	.01	**0.24**	−.25	0.50	.01	**0.24**
SLF III right	.08	**0.26**	.20	0.39	−.07	**0.25**	−.05	**0.25**	−.10	**0.27**	.02	**0.24**
Cingulate left	−.20	0.39	−.17	0.33	−.35	1.05	−.11	**0.27**	−.37	1.39	−.03	**0.24**
Cingulate right	.00	**0.24**	.04	**0.24**	−.33	0.95	−.18	0.35	−.27	0.56	.13	**0.29**
PLIC left	−.20	0.38	.05	**0.25**	−.17	0.34	.16	0.33	−.29	0.67	−.25	0.51
PLIC right	−.14	**0.30**	.11	**0.28**	.09	**0.26**	.23	0.46	.04	**0.24**	−.19	0.37
DLPFC left	.01	**0.24**	.21	0.40	.04	**0.24**	.12	**0.28**	−.06	**0.25**	−.18	0.35
DLPFC right	−.29	0.67	−.26	0.52	−.20	0.38	−.05	**0.25**	−.27	0.57	−.09	**0.26**
Splenium CC	−.30	0.74	−.23	0.46	−.07	**0.25**	.17	0.33	−.09	**0.26**	−.08	**0.26**

Note. Inverse Bayes factors (BF_{10}) supporting the H_0 (i.e., < 0.33) are presented in boldface, while those supporting the H_1 (i.e., > 3) are presented in boldface and underlined. SLF = superior longitudinal fasciculus, PLIC = posterior limb of internal capsule, DLPFC = dorsolateral prefrontal caudate, CC = corpus callosum, RT = reaction time, SD = standard deviation, A′ = non-parametric index of sensitivity, B″ = non-parametric index of response bias, *r* = Pearson correlation, BF = Bayes Factor.

stronger evidence in favor of the H_1 by the Bayesian analysis.

4. Discussion

The main goal of the present study was to provide further evidence to dissociate the structural brain connectivity underlying the functioning of the attentional networks in healthy adults. To this end, we offline correlated the performance scores of the classic attentional components and EV obtained across two experimental sessions with the ANTI-V task [40] with the microstructure connectivity of white matter tracts previously associated with attentional performance [20–22,24,36]. It is important to highlight that the methodological procedure and statistical analyses conducted in the present study aimed at solving some critical limitations observed in previous research. First, we used a fine-grained behavioral paradigm that provides in a single session an independent measure of the classic attentional components and EV: the ANTI-V [40]. Furthermore, we reconstructed DWI data with the spherical deconvolutions approach [34,45,46], a methodology that is much sensitive for dissecting white matter tracts that are embedded in brain regions with crossing fibers, as the SLFs [21]. Thus, we computed the HMOA index for analyzing white matter connectivity, which is indeed a more appropriate index for measuring the diffusion properties in white matter regions with a complex organization than the traditional FA index [34]. Lastly, we used two statistical analyses to interpret the outcomes: whereas Pearson correlations were computed to analyze the evidence supporting rejection of the null hypothesis (i.e., there is no correlation between performance scores and white matter connectivity), we also computed Bayesian correlations for analyzing the evidence gathered for supporting either the absence or the existence of a correlation.

Importantly, the main effects and interactions for the classic attentional components and the EV indices [40,41], the test-retest reliability of performance scores [11,42], and the expected hemispheric lateralization (if any) of the targeted white matters tracts [21,22,58,59] were observed in the same vein as previous outcomes, therefore validating the present methods and the observed correlations between performance scores and white matter connectivity. Concerning the correlations between HMOA indices and the attentional/vigilance performance, it is also important to note that some relative large Pearson correlations were however not observed at least by positive evidence in favor of the existence of correlation by the Bayesian analysis (e.g., the RT phasic alertness score from no cue trials with the left DLPFC; although showing an unexpected positive correlation). Moreover, some non-significant correlations showed a BF_{10} between 1 and 3, thus suggesting only anecdotal evidence to the H_1 (e.g., the RT orienting score with the right SLF III). Therefore, the actual existence of these non-significant correlations should be effectively determined either by collecting a larger sample size than the one used in the present study or by metanalytic evidence considering the different studies, to gather a much larger amount of evidence for those correlations [61].

However, beyond that potential limitation, taking into consideration those findings with at least positive evidence for the existence of correlation by the Bayesian analysis, we observed reliable outcomes that might be summarized as: (a) a higher HMOA index in the left cingulate fasciculus was associated with faster overall responses in attentional networks performance; (b) higher HMOA indices in the right DLPFC and the splenium of the CC were related to a reduced effect of phasic alertness (for the errors score); (c) higher HMOA indices in bilateral SLF I were associated with faster responses for the correct detection of infrequent signals in EV performance; and (d) critically, no relevant correlations were observed for the overall of errors in the ANTI trials, the orienting scores, the executive control performance, and the signal-detection theory metrics computed for EV.

It is interesting to note that two of the three scores that showed relevant correlations with white matter tracts connectivity were the overall RT for the attentional networks' performance (i.e., ANTI trials) and the overall RT for the EV task, which are indeed the most reliable performance scores usually observed with the ANT, ANTI, or ANTI-V tasks [11,12,42]. Therefore, it might be reasonable to think that those performance scores that are more reliable and stable across experimental sessions are the ones that correlate with white matter microstructural connectivity. In this vein, it has been proved that white matter connectivity is strongly related to long term stable changes, as maturation [62], training [63], or the structural damage linked to diseases as stroke, attention-deficit/hyperactivity disorder, schizophrenia, or multiple sclerosis [27,29,64–66].

However, this reasoning does not seem to fit well with the strong and independent correlation observed between the HMOA indices of both the right DLPFC and the splenium of the CC with the phasic alertness score, which is indeed an attentional component classically interpreted as an attentional state rather than a stable trait [11]. To account for this latter outcome, nevertheless, we might contemplate at last two main considerations: (a) although phasic alertness refers to a short term process that shows moderate-to-low reliability in the present study and also in previous studies with the ANT [11] or ANTI-V [42], the phasic alertness scores (both for RT and errors) demonstrated both considerable stability when it was assessed with the ANTI task across 10 consecutive sessions and moderate-to-high split-half reliability (i.e., .70 for the errors score) when it was computed considering the data of these 10 sessions [12]; and (b) the right DLPFC and the splenium of the CC effectively connects brain regions underlying the alerting network circuit, i.e., brain stem regions as the locus coeruleus along with prefrontal and parietal cortices [1,26]. Notwithstanding, although this finding might be quite relevant for disentangling the underlying white matter connectivity of the alerting network, we reckon that further research supporting this novel evidence is imperatively necessary.

On the other hand, although we observed a relevant correlation between the bilateral SLF I connectivity and the overall mean RT for the EV task, consistent with previous evidence on the role of the SLF in sustained attention [36,67,68], the signal-detection theory metrics –which are indeed the most descriptive indices of EV as the ability to detect infrequent critical signals over long periods [69,70]– showed no correlations with white matter tracts connectivity, despite these indices showing larger reliability scores. To account for this inconsistent outcome, it might be relevant to take into account some limitations of the ANTI-V task on the assessment of EV. Although the signal-detection theory scores computed here and in previous research [42] showed high reliability, the EV task embedded in the ANTI-V task is indeed a signal detection task quite difficult to perform. Thus, the hits rate observed here (i.e., 46 % overall across sessions) is similar to the one observed in previous studies with the ANTI-V, wherein it was found between 45 % and 60 % as maximum [40,43,44,71–73]. Furthermore, and most importantly, the above-cited studies with the ANTI-V have not reported the decrement of performance across time-on-task, i.e., the typical phenomenon usually observed in vigilance tasks [74]. In this vein, when either the RT or signal-detection theory metrics of the present study are analyzed comparing the performance across time-on-task (i.e., by experimental blocks), the repeated-measures ANOVAs show indeed no significant shift across blocks (all $Fs < 1.16$, $ps > .330$).

Future research aiming at examining the structural connectivity underlying the human attentional networks and especially vigilance processes might consider using the newest version of the ANT: the ANT for Interactions and Vigilance – executive and arousal components (ANTI-Vea) [75]. The ANTI-Vea is suitable to assess the independence and interactions of the classic attentional components as in the ANTI [41], but (at the same time), it provides an independent and direct measure of two vigilance components: (a) the EV, as the ability to detect infrequent critical signals; and (b) the arousal vigilance (AV), a component usually assessed in the Psychomotor Vigilance Test [76] as the capacity to sustain across time-on-task a fast reaction to stimuli from the environment without implementing much control [75]. Note that, importantly, the ANTI-Vea solves the above-mentioned issues of the ANTI-V task: (a) the EV task is easier to perform, as observed in the

overall hits rate of ~75 %; and (b) the task is suitable to observe the decrement across time-on-task for both the EV and AV components [75,77]. Thus, it might be expected that a behavioral task suitable to assess the vigilance decrement phenomenon, which is the behavioral pattern by definition of vigilance [74,78], could also be indeed more sensitive to reflect potential implications of white matter tracts connectivity underlying the attentional network system.

Finally, we did not replicate previous findings supporting relevant associations between: (a) the orienting functioning and the splenium of the CC [20] and/or the SLF III [21,24]; (b) executive control processes and the left DLPFC [22]; and (c) the EV component and the left cingulate fasciculus [36] and/or the right DLPFC [22]. As above-mentioned, Bayesian analyses demonstrated that the evidence accumulated here was weak or anecdotal to support the existence of correlations between the RT score of orienting and the SLF III, and the left DLPFC and the RT score of executive control (although in this last case the potential correlation was unexpectedly positive). Furthermore, the correlations between the splenium of the CC and RT score of orienting, and sensitivity with either the right DLPFC or the right cingulate, were observed as inconsistent evidence to support either the H_0 or the H_1.

Nevertheless, to further account for this set of above-mentioned non-replicated outcomes, we might also consider some differences between the present study and the previous ones. Regarding the behavioral task, note that Niogi et al. [20] assessed the classic attentional components by using the ANT, which presents a different cueing paradigm for measuring phasic alertness and orienting than the ANTI [41] and the ANTI-V [40]. In particular, whereas in the ANT task the orienting cue is 100 % predictive of the target location, therefore involving endogenous orienting, in the ANTI task the cue is completely unpredictive, thus rather involving exogenous orienting. Regarding the score computed for measuring white matter structural connectivity, it might be probable that some previous outcomes obtained by using the FA index, as those reported by Niogi et al. [20] and Chiang et al. [22], would not be successfully replicated by using the most sensitive HMOA index. Interestingly, note also that the control healthy participants from the study by Chiang et al. [22] were young participants between 7 and 18 years old, and so, it might be highly probable that some differences with those outcomes would be linked to maturation factors [62]. Nevertheless, beyond these interpretative considerations, we reckon that further evidence is critically necessary to disentangle these inconsistent outcomes.

5. Conclusions

To conclude, the present study aimed at examining and dissociating the white matter connectivity underlying the human attentional networks in the healthy brain. We found consistent evidence concerning the right DLPFC and the splenium of the CC as associated with the alerting network. Regarding the expected role of the right SLF III in the orienting network and the left DLPFC tract in the executive control network, the evidence collected in the present study seemed to be weak for supporting these correlations, and no further relevant correlations were observed for neither orienting nor executive control. Besides, the signal-detection theory scores of EV –which are the most informative indices regarding the ability to detect infrequent signals over long time periods– were not associated in the present study with the right cingulate and right DLPFC, at difference with previously reported outcomes. However, interestingly, white matter connectivity seems to support performance reliability: whereas the left cingulate was associated with the mean overall RT of attentional networks performance, bilateral SLF I was associated with the overall RT of EV performance. Despite these consistent outcomes, we reckon that further evidence is critically necessary to support the discussions provided here, and most importantly, to achieve a consensus regarding the structural connectivity underlying human attentional networks.

Data statement

The dataset analyzed in the present study are publicly available in the Open Science Framework (https://osf.io/6qvzk/)

CRediT authorship contribution statement

Fernando G. Luna: Conceptualization, Methodology, Software, Validation, Formal analysis, Investigation, Data curation, Writing - original draft, Visualization. **Juan Lupiáñez:** Conceptualization, Validation, Resources, Writing - review & editing, Project administration, Funding acquisition. **Elisa Martín-Arévalo:** Conceptualization, Validation, Formal analysis, Writing - review & editing, Supervision.

Declaration of Competing Interest

The authors declare that they have no known competing financial interests or personal relationships that could have appeared to influence the work reported in this paper.

Acknowledgments

This work was supported by the Spanish Ministry of Economy, Industry, and Competitiveness, through research projects to JL [grant number PSI2014-52764-P and PSI2017-84926-P]. FGL received PhD scholarship support from the Consejo Nacional de Investigaciones Científicas y Técnicas (CONICET), Argentina. Funding's institutions had no involvement in study design; in the collection, analysis and interpretation of data; in the writing of the report; nor in the decision to submit the article for publication. This paper is part of the doctoral dissertation of FGL, conducted under the supervision of JL and EMA.

References

[1] S.E. Petersen, M.I. Posner, The attention system of the human brain: 20 years after, Annu. Rev. Neurosci. 35 (2012) 73–89, https://doi.org/10.1146/annurev-neuro-062111-150525.
[2] M.I. Posner, S.E. Petersen, The attention system of the human brain, Annu. Rev. Neurosci. 13 (1990) 25–42, https://doi.org/10.1146/annurev.ne.13.030190.000325.
[3] M.I. Posner, S. Dehaene, Attentional networks, Trends Neurosci. 17 (1994) 75–79, https://doi.org/10.1016/0166-2236(94)90078-7.
[4] M.I. Posner, Measuring alertness, Ann. N. Y. Acad. Sci. 1129 (2008) 193–199, https://doi.org/10.1196/annals.1417.011.
[5] M.I. Posner, Orienting of attention: then and now, Q. J. Exp. Psychol. 69 (2016) 1864–1875, https://doi.org/10.1080/17470218.2014.937446.
[6] A. Shenhav, M.M. Botvinick, J.D. Cohen, The expected value of control: an integrative theory of anterior cingulate cortex function, Neuron 79 (2013) 217–240, https://doi.org/10.1016/j.neuron.2013.07.007.
[7] M.M. Botvinick, J.D. Cohen, C.S. Carter, Conflict monitoring and anterior cingulate cortex: an update, Trends Cogn. Sci. 8 (2004) 539–546, https://doi.org/10.1016/j.tics.2004.10.003.
[8] J. Fan, B.D. McCandliss, T. Sommer, A. Raz, M.I. Posner, Testing the efficiency and independence of attentional networks, J. Cogn. Neurosci. 14 (2002) 340–347, https://doi.org/10.1162/089892902317361886.
[9] M.I. Posner, Orienting of attention, Q. J. Exp. Psychol. 32 (1980) 3–25, https://doi.org/10.1080/00335558008248231.
[10] B.A. Eriksen, C.W. Eriksen, Effects of noise letters upon the identification of a target letter in a nonsearch task, Percept. Psychophys. 16 (1974) 143–149, https://doi.org/10.3758/BF03203267.
[11] J.W. MacLeod, M.A. Lawrence, M.M. McConnell, G.A. Eskes, R.M. Klein, D.I. Shore, Appraising the ANT: psychometric and theoretical considerations of the attention network test, Neuropsychology 24 (2010) 637–651, https://doi.org/10.1037/a0019803.
[12] Y. Ishigami, R.M. Klein, Repeated measurement of the components of attention using two versions of the Attention Network Test (ANT): stability, isolability, robustness, and reliability, J. Neurosci. Methods 190 (2010) 117–128, https://doi.org/10.1016/j.jneumeth.2010.04.019.
[13] B. Xuan, M.A. Mackie, A. Spagna, T. Wu, Y. Tian, P.R. Hof, J. Fan, The activation of interactive attentional networks, Neuroimage 129 (2016) 308–319, https://doi.org/10.1016/j.neuroimage.2016.01.017.
[14] J. Fan, B.D. McCandliss, J. Fossella, J.I. Flombaum, M.I. Posner, The activation of attentional networks, Neuroimage 26 (2005) 471–479, https://doi.org/10.1016/j.neuroimage.2005.02.004.
[15] A. Galvao-Carmona, J.J. González-Rosa, A.R. Hidalgo-Muñoz, D. Páramo, M. L. Benítez, G. Izquierdo, M. Vázquez-Marrufo, Disentangling the attention network

test: behavioral, event related potentials, and neural source analyses, Front. Hum. Neurosci. 8 (2014) 1–16, https://doi.org/10.3389/fnhum.2014.00813.
[16] A.H. Neuhaus, C. Urbanek, C. Opgen-Rhein, E. Hahn, T.M.T. Ta, S. Koehler, M. Gross, M. Dettling, Event-related potentials associated with attention network test, Int. J. Psychophysiol. 76 (2010) 72–79, https://doi.org/10.1016/j.ijpsycho.2010.02.005.
[17] A. Abundis-Gutiérrez, P. Checa, C. Castellanos, M. Rosario Rueda, Electrophysiological correlates of attention networks in childhood and early adulthood, Neuropsychologia 57 (2014) 78–92, https://doi.org/10.1016/j.neuropsychologia.2014.02.013.
[18] A. Raz, J. Buhle, Typologies of attentional networks, Nat. Rev. Neurosci. 7 (2006) 367–379, https://doi.org/10.1038/nrn1903.
[19] C.M. Thiel, K. Zilles, G.R. Fink, Cerebral correlates of alerting, orienting and reorienting of visuospatial attention: an event-related fMRI study, Neuroimage 21 (2004) 318–328, https://doi.org/10.1016/j.neuroimage.2003.08.044.
[20] S. Niogi, P. Mukherjee, J. Ghajar, B.D. McCandliss, Individual differences in distinct components of attention are linked to anatomical variations in distinct white matter tracts, Front. Neuroanat. 4 (2010) 1–12, https://doi.org/10.3389/neuro.05.002.2010.
[21] M. Thiebaut de Schotten, F. Dell'Acqua, S.J. Forkel, A. Simmons, F. Vergani, D.G. M. Murphy, M. Catani, A lateralized brain network for visuospatial attention, Nat. Neurosci. 14 (2011) 1245–1246, https://doi.org/10.1038/nn.2905.
[22] H.-L. Chiang, Y.-J. Chen, Y.-C. Lo, W.-Y.I. Tsen, S.S.-F. Gau, Altered white matter tract property related to impaired focused attention, sustained attention, cognitive impulsivity and vigilance in attention-deficit/ hyperactivity disorder, J. Psychiatry Neurosci. 40 (2015) 325–335, https://doi.org/10.1503/jpn.140106.
[23] X. Yin, Y. Han, H. Ge, W. Xu, R. Huang, D. Zhang, J. Xu, L. Fan, Z. Pang, S. Liu, Inferior frontal white matter asymmetry correlates with executive control of attention, Hum. Brain Mapp. 34 (2013) 796–813, https://doi.org/10.1002/hbm.21477.
[24] H. Ge, X. Yin, J. Xu, Y. Tang, Y. Han, W. Xu, Z. Pang, H. Meng, S. Liu, Fiber pathways of attention subnetworks revealed with tract-based spatial statistics (TBSS) and probabilistic tractography, PLoS One 8 (2013), e78831, https://doi.org/10.1371/journal.pone.0078831.
[25] M.I. Posner, B.E. Sheese, Y. Odludaş, Y. Tang, Analyzing and shaping human attentional networks, Neural Netw. 19 (2006) 1422–1429, https://doi.org/10.1016/j.neunet.2006.08.004.
[26] M.I. Posner, Imaging attention networks, Neuroimage 61 (2012) 450–456, https://doi.org/10.1016/j.neuroimage.2011.12.040.
[27] S.J. Forkel, P. Friedrich, M. Thiebaut de Schotten, H. Howells, White matter variability, cognition, and disorders: a systematic review, MedRxiv 2020 (2020), https://doi.org/10.1101/2020.04.22.20075127, 04.22.20075127.
[28] D.K. Jones, A. Leemans, Diffusion tensor imaging, Methods Mol. Biol. 711 (2011) 127–144, https://doi.org/10.1007/978-1-61737-992-5_6.
[29] D. Le Bihan, J.-F. Mangin, C. Poupon, C. a Clark, S. Pappata, N. Molko, H. Chabriat, Diffusion tensor imaging: concepts and applications, J. Magn. Reson. Imaging 13 (2001) 534–546, https://doi.org/10.1002/jmri.1076.
[30] M. Catani, M. Thiebaut de Schotten, A diffusion tensor imaging tractography atlas for virtual in vivo dissections, Cortex 44 (2008) 1105–1132, https://doi.org/10.1016/j.cortex.2008.05.004.
[31] A.B. Chica, M. Thiebaut de Schotten, P. Bartolomeo, P.M. Paz-Alonso, White matter microstructure of attentional networks predicts attention and consciousness functional interactions, Brain Struct. Funct. 223 (2018) 653–668, https://doi.org/10.1007/s00429-017-1511-2.
[32] C. Beaulieu, The basis of anisotropic water diffusion in the nervous system - a technical review, NMR Biomed. 15 (2002) 435–455, https://doi.org/10.1002/nbm.782.
[33] J.M. Soares, P. Marques, V. Alves, N. Sousa, A hitchhiker's guide to diffusion tensor imaging, Front. Neurosci. 7 (2013) 31, https://doi.org/10.3389/fnins.2013.00031.
[34] F. Dell'Acqua, A. Simmons, S.C.R. Williams, M. Catani, Can spherical deconvolution provide more information than fiber orientations? Hindrance modulated orientational anisotropy, a true-tract specific index to characterize white matter diffusion, Hum. Brain Mapp. 34 (2013) 2464–2483, https://doi.org/10.1002/hbm.22080.
[35] C. Conners, Conners' Continuous Performance Test I.I., Multi-Health Systems, Toronto, Canada, 2000.
[36] M. Takahashi, K. Iwamoto, H. Fukatsu, S. Naganawa, T. Iidaka, N. Ozaki, White matter microstructure of the cingulum and cerebellar peduncle is related to sustained attention and working memory: a diffusion tensor imaging study, Neurosci. Lett. 477 (2010) 72–76, https://doi.org/10.1016/j.neulet.2010.04.031.
[37] N. Makris, D.N. Kennedy, S. McInerney, G. Sorensen, R. Wang, V.S. Caviness, D. N. Pandya, Segmentation of subcomponents within the superior longitudinal fascicle in humans: a quantitative, in vivo, DT-MRI study, Cereb. Cortex 15 (2005) 854–869, https://doi.org/10.1093/cercor/bhh186.
[38] M. Corbetta, G. Patel, G.L. Shulman, The reorienting system of the human brain: from environment to theory of mind, Neuron 58 (2008) 306–324, https://doi.org/10.1016/j.neuron.2008.04.017.
[39] A.B. Chica, P. Bartolomeo, J. Lupiáñez, Two cognitive and neural systems for endogenous and exogenous spatial attention, Behav. Brain Res. 237 (2013) 107–123, https://doi.org/10.1016/j.bbr.2012.09.027.
[40] J. Roca, C. Castro, M.F. López-Ramón, J. Lupiáñez, Measuring vigilance while assessing the functioning of the three attentional networks: the ANTI-Vigilance task, J. Neurosci. Methods 198 (2011) 312–324, https://doi.org/10.1016/j.jneumeth.2011.04.014.
[41] A. Callejas, J. Lupiáñez, P. Tudela, The three attentional networks: on their independence and interactions, Brain Cogn. 54 (2004) 225–227, https://doi.org/10.1016/j.bandc.2004.02.012.
[42] J. Roca, P. García-Fernández, C. Castro, J. Lupiáñez, The moderating effects of vigilance on other components of attentional functioning, J. Neurosci. Methods 308 (2018) 151–161, https://doi.org/10.1016/j.jneumeth.2018.07.019.
[43] J. Roca, L.J. Fuentes, A. Marotta, M.-F. López-Ramón, C. Castro, J. Lupiáñez, D. Martella, The effects of sleep deprivation on the attentional functions and vigilance, Acta Psychol. (Amst.) 140 (2012) 164–176, https://doi.org/10.1016/j.actpsy.2012.03.007.
[44] A. Marotta, R.D. Chiaie, A. Spagna, L. Bernabei, M. Sciarretta, J. Roca, M. Biondi, M. Casagrande, Impaired conflict resolution and vigilance in euthymic bipolar disorder, Psychiatry Res. 229 (2015) 490–496, https://doi.org/10.1016/j.psychres.2015.06.026.
[45] D.C. Alexander, Multiple-fiber reconstruction algorithms for diffusion MRI, Ann. N. Y. Acad. Sci. 1064 (2005) 113–133, https://doi.org/10.1196/annals.1340.018.
[46] J.-D. Tournier, F. Calamante, D.G. Gadian, A. Connelly, Direct estimation of the fiber orientation density function from diffusion-weighted MRI data using spherical deconvolution, Neuroimage 23 (2004) 1176–1185, https://doi.org/10.1016/j.neuroimage.2004.07.037.
[47] M. Catani, M. Thiebaut de Schotten, Atlas of Human Brain Connections, Oxford University Press, New York, 2012.
[48] A. Leemans, B. Jeurissen, J. Sijbers, D.K. Jones, ExploreDTI: a graphical toolbox for processing, analyzing, and visualizing diffusion MR data, in: 17th Annu. Meet. Intl Soc Mag Reson Med, Hawaii, 2009, p. 3537.
[49] R. Wang, T. Benner, A.G. Sorensen, V.J. Wedeen, Diffusion toolkit: a software package for diffusion imaging data processing and tractography, in: 15th Annu. Meet. Intl Soc Mag Reson Med, Berlin, 2007, p. 3720.
[50] K. Rojkova, E. Volle, M. Urbanski, F. Humbert, F. Dell'Acqua, M. Thiebaut de Schotten, Atlasing the frontal lobe connections and their variability due to age and education: a spherical deconvolution tractography study, Brain Struct. Funct. 221 (2016) 1751–1766, https://doi.org/10.1007/s00429-015-1001-3.
[51] Psychology Software Tools, Inc. [E-Prime 2.0] 2012; http://www.pstnet.com.
[52] StatSoft, Inc, STATISTICA (Data Analyses Software System), Version 8.0, 2007. http://www.statsoft.com.
[53] JASP Team, JASP (Version 0.13.1), 2019. https://jasp-stats.org/.
[54] E.-J. Wagenmakers, J. Love, M. Marsman, T. Jamil, A. Ly, J. Verhagen, R. Selker, Q. F. Gronau, D. Dropmann, B. Boutin, F. Meerhoff, P. Knight, A. Raj, E.-J. van Kesteren, J. van Doorn, M. Šmíra, S. Epskamp, A. Etz, D. Matzke, T. de Jong, D. van den Bergh, A. Sarafoglou, H. Steingroever, K. Derks, J.N. Rouder, R.D. Morey, Bayesian inference for psychology. Part II: example applications with JASP, Psychon. Bull. Rev. 25 (2018) 58–76, https://doi.org/10.3758/s13423-017-1323-7.
[55] A. Callejas, J. Lupiáñez, M.J. Funes, P. Tudela, Modulations among the alerting, orienting and executive control networks, Exp. Brain Res. 167 (2005) 27–37, https://doi.org/10.1007/s00221-005-2365-z.
[56] J.B. Grier, Nonparametric indexes for sensitivity and bias: computing formulas, Psychol. Bull. 75 (1971) 424–429, https://doi.org/10.1037/h0031246.
[57] D. Cousineau, Confidence intervals in within-subject designs: a simpler solution to Loftus and Masson's method, Tutor. Quant. Methods Psychol. 1 (2005) 42–45, https://doi.org/10.20982/tqmp.01.1.p042.
[58] G. Gong, T. Jiang, C. Zhu, Y. Zang, F. Wang, S. Xie, J. Xiao, X. Guo, Asymmetry analysis of cingulum based on scale-invariant parameterization by diffusion tensor imaging, Hum. Brain Mapp. 24 (2005) 92–98, https://doi.org/10.1002/hbm.20072.
[59] H. Takao, N. Hayashi, K. Ohtomo, White matter asymmetry in healthy individuals: a diffusion tensor imaging study using tract-based spatial statistics, Neuroscience 193 (2011) 291–299, https://doi.org/10.1016/j.neuroscience.2011.07.041.
[60] A.F. Jarosz, J. Wiley, What are the odds? A practical guide to computing and reporting bayes factors, J. Probl. Solving 7 (2014) 2–9, https://doi.org/10.7771/1932-6246.1167.
[61] M.E.J. Masson, A tutorial on a practical Bayesian alternative to null-hypothesis significance testing, Behav. Res. Methods 43 (2011) 679–690, https://doi.org/10.3758/s13428-010-0049-5.
[62] C. Lebel, L. Walker, A. Leemans, L. Phillips, C. Beaulieu, Microstructural maturation of the human brain from childhood to adulthood, Neuroimage 40 (2008) 1044–1055, https://doi.org/10.1016/j.neuroimage.2007.12.053.
[63] J. Scholz, M.C. Klein, T.E.J. Behrens, H. Johansen-Berg, Training induces changes in white-matter architecture, Nat. Neurosci. 12 (2009) 1370–1371, https://doi.org/10.1038/nn.2412.
[64] A. Bourgeois, A.B. Chica, R. Migliaccio, M.T. de Schotten, P. Bartolomeo, Cortical control of inhibition of return: evidence from patients with inferior parietal damage and visual neglect, Neuropsychologia 50 (2012) 800–809, https://doi.org/10.1016/j.neuropsychologia.2012.01.014.
[65] F. Doricchi, M. Thiebaut de Schotten, F. Tomaiuolo, P. Bartolomeo, White matter (dis)connections and gray matter (dys)functions in visual neglect: gaining insights into the brain networks of spatial awareness, Cortex 44 (2008) 983–995, https://doi.org/10.1016/j.cortex.2008.03.006.
[66] H. van Ewijk, D.J. Heslenfeld, M.P. Zwiers, J.K. Buitelaar, J. Oosterlaan, Diffusion tensor imaging in attention deficit/hyperactivity disorder: a systematic review and meta-analysis, Neurosci. Biobehav. Rev. 36 (2012) 1093–1106, https://doi.org/10.1016/j.neubiorev.2012.01.003.
[67] B. Klarborg, K. Skak Madsen, M. Vestergaard, A. Skimminge, T.L. Jernigan, W.F. C. Baaré, Sustained attention is associated with right superior longitudinal fasciculus and superior parietal white matter microstructure in children, Hum. Brain Mapp. 34 (2013) 3216–3232, https://doi.org/10.1002/hbm.22139.

[68] A. Konrad, T.F. Dielentheis, D. El Masri, M. Bayerl, C. Fehr, T. Gesierich, G. Vucurevic, P. Stoeter, G. Winterer, Disturbed structural connectivity is related to inattention and impulsivity in adult attention deficit hyperactivity disorder, Eur. J. Neurosci. 31 (2010) 912–919, https://doi.org/10.1111/j.1460-9568.2010.07110.x.

[69] D.R. Thomson, D. Besner, D. Smilek, A critical examination of the evidence for sensitivity loss in modern vigilance tasks, Psychol. Rev. 123 (2016) 70–83, https://doi.org/10.1037/rev0000021.

[70] H. Stanislaw, N. Todorov, Calculation of signal detection theory measures, Behav. Res. Methods Instrum. Comput. 31 (1999) 137–149, https://doi.org/10.3758/BF03207704.

[71] J. Roca, J. Lupiáñez, M.-F. López-Ramón, C. Castro, Are drivers' attentional lapses associated with the functioning of the neurocognitive attentional networks and with cognitive failure in everyday life? Transp. Res. Part F Traffic Psychol. Behav. 17 (2013) 98–113, https://doi.org/10.1016/j.trf.2012.10.005.

[72] J. Roca, D. Crundall, S. Moreno-Ríos, C. Castro, J. Lupiáñez, The influence of differences in the functioning of the neurocognitive attentional networks on drivers' performance, Accid. Anal. Prev. 50 (2013) 1193–1206, https://doi.org/10.1016/j.aap.2012.09.032.

[73] J. Morales, F. Padilla, C.J. Gómez-Ariza, M.T. Bajo, Simultaneous interpretation selectively influences working memory and attentional networks, Acta Psychol. (Amst.) 155 (2015) 82–91, https://doi.org/10.1016/j.actpsy.2014.12.004.

[74] P.A. Hancock, On the nature of vigilance, Hum. Factors 59 (2017) 35–43, https://doi.org/10.1177/0018720816655240.

[75] F.G. Luna, J. Marino, J. Roca, J. Lupiáñez, Executive and arousal vigilance decrement in the context of the attentional networks: the ANTI-Vea task, J. Neurosci. Methods 306 (2018) 77–87, https://doi.org/10.1016/j.jneumeth.2018.05.011.

[76] J. Lim, D.F. Dinges, Sleep deprivation and vigilant attention, Ann. N. Y. Acad. Sci. 1129 (2008) 305–322, https://doi.org/10.1196/annals.1417.002.

[77] F.G. Luna, R. Román-Caballero, P. Barttfeld, J. Lupiáñez, E. Martín-Arévalo, A high-definition tDCS and EEG study on attention and vigilance: brain stimulation mitigates the executive but not the arousal vigilance decrement, Neuropsychologia 142 (2020), 107447, https://doi.org/10.1016/j.neuropsychologia.2020.107447.

[78] N.H. Mackworth, The breakdown of vigilance during prolonged visual search, Q. J. Exp. Psychol. 1 (1948) 6–21, https://doi.org/10.1080/17470214808416738.